

## Supporting Information

for

### Highly phase-separated alternating copolymer of alkyl vinyl ether and sulfonic acid group-containing trifluoro vinyl ether

Kaishi Hori<sup>a</sup> Shoji Miyanishi<sup>b</sup> and Takeo Yamaguchi<sup>b</sup>

<sup>a</sup>Laboratory of Advanced Science & Technology, Corporate Research & Development, Asahi Kasei Corporation, 2-1 Samejima, Fuji, Shizuoka, 416-8501, Japan

<sup>b</sup>Laboratory for Chemistry and Life Science Institute of Innovative Research, Science Tokyo, R1-17, 4259, Midori-ku, Yokohama, Kanagawa, 226-8503, Japan

Corresponding author: yamag@res.titech.ac.jp

#### Contents

Figure S1. <sup>1</sup>H-NMR (top) and <sup>19</sup>F-NMR (bottom) spectra of C<sub>2</sub>-SO<sub>2</sub>F

Figure S2. <sup>1</sup>H-NMR (top) and <sup>19</sup>F-NMR (bottom) spectra of C<sub>4</sub>-SO<sub>2</sub>F

Figure S3. <sup>1</sup>H-NMR (top) and <sup>19</sup>F-NMR (bottom) spectra of C<sub>12</sub>-SO<sub>2</sub>F

Figure S4. <sup>1</sup>H-NMR (top) and <sup>19</sup>F-NMR (bottom) spectra of C<sub>18</sub>-SO<sub>2</sub>F

Figure S5. <sup>1</sup>H-NMR (top) and <sup>19</sup>F-NMR (bottom) spectra of C<sub>2</sub>-SO<sub>3</sub>Li

Figure S6. <sup>1</sup>H-NMR (top) and <sup>19</sup>F-NMR (bottom) spectra of C<sub>4</sub>-SO<sub>3</sub>Li

Figure S7. <sup>1</sup>H-NMR (top) and <sup>19</sup>F-NMR (bottom) spectra of C<sub>12</sub>-SO<sub>3</sub>Li

Figure S8. <sup>1</sup>H-NMR (top) and <sup>19</sup>F-NMR (bottom) spectra of C<sub>18</sub>-SO<sub>3</sub>Li

Figure S9. <sup>1</sup>H-NMR (top) and <sup>19</sup>F-NMR (bottom) spectra of C<sub>2</sub>-SO<sub>3</sub>Cs

Figure S10. <sup>1</sup>H-NMR (top) and <sup>19</sup>F-NMR (bottom) spectra of C<sub>4</sub>-SO<sub>3</sub>Cs

Figure S11. <sup>1</sup>H-NMR (top) and <sup>19</sup>F-NMR (bottom) spectra of C<sub>12</sub>-SO<sub>3</sub>Cs

Figure S12. <sup>1</sup>H-NMR (top) and <sup>19</sup>F-NMR (bottom) spectra of C<sub>18</sub>-SO<sub>3</sub>Cs

Figure S13. <sup>1</sup>H-NMR (top) and <sup>19</sup>F-NMR (bottom) spectra of C<sub>2</sub>-SO<sub>3</sub>H

Figure S14. <sup>1</sup>H-NMR (top) and <sup>19</sup>F-NMR (bottom) spectra of C<sub>4</sub>-SO<sub>3</sub>H

Figure S15. <sup>1</sup>H-NMR (top) and <sup>19</sup>F-NMR (bottom) spectra of C<sub>12</sub>-SO<sub>3</sub>H

Figure S16. <sup>1</sup>H-NMR (top) and <sup>19</sup>F-NMR (bottom) spectra of C<sub>18</sub>-SO<sub>3</sub>H

Figure S17. Figure S17. 2D Fourier transfer of TEM bright field image (right) and its strength profile (left) of C<sub>12</sub>-SO<sub>3</sub>Li

Figure S18. Figure S17. 2D Fourier transfer of TEM bright field image (right) and its strength profile

(left) of C<sub>18</sub>-SO<sub>3</sub>Li

Figure S19. PFG-NMR diffusion plot of C<sub>2</sub>-SO<sub>3</sub>H (a), C<sub>4</sub>-SO<sub>3</sub>H (b), C<sub>12</sub>-SO<sub>3</sub>H (c) and C<sub>18</sub>-SO<sub>3</sub>H (d)

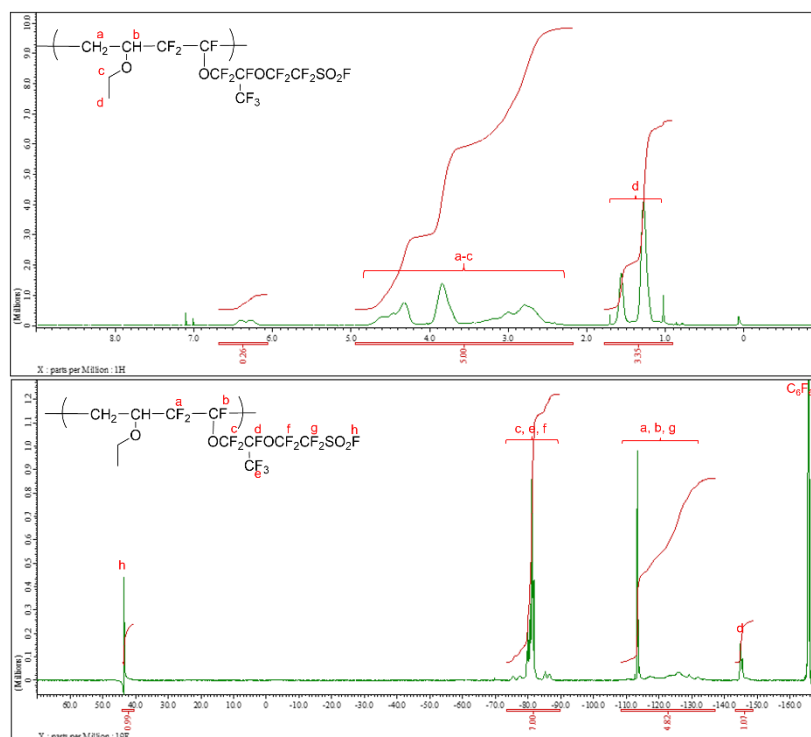


Figure S1. <sup>1</sup>H-NMR (top) and <sup>19</sup>F-NMR (bottom) spectra of C<sub>2</sub>-SO<sub>2</sub>F

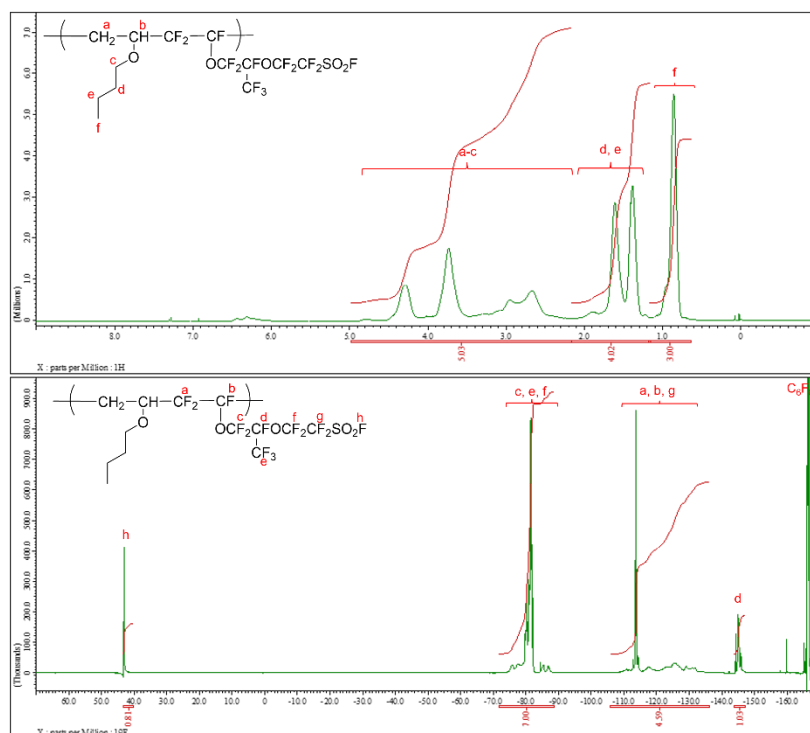


Figure S2.  $^1\text{H}$ -NMR (top) and  $^{19}\text{F}$ -NMR (bottom) spectra of  $\text{C}_4\text{-SO}_2\text{F}$

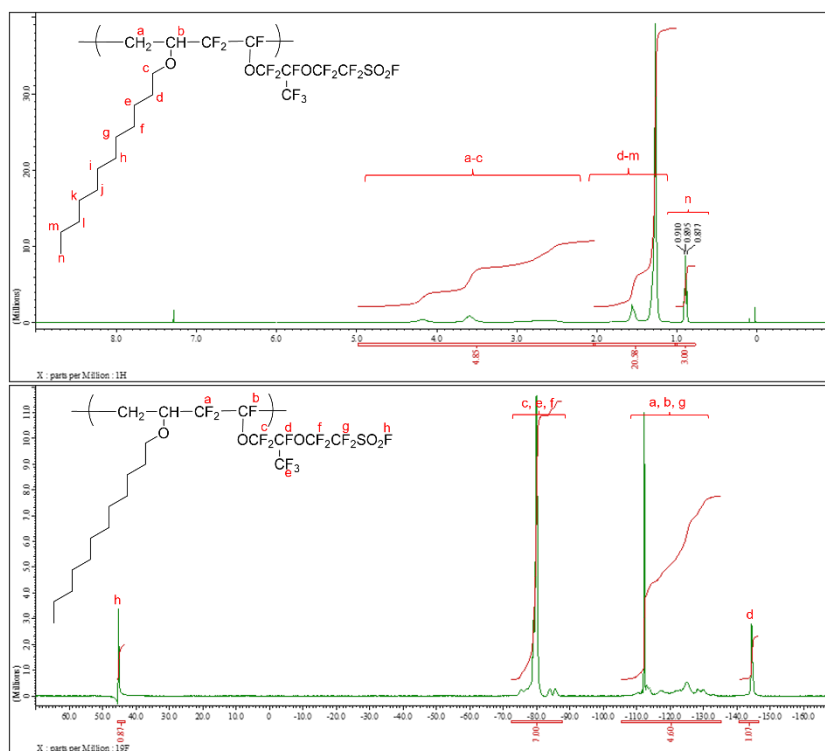


Figure S3.  $^1\text{H}$ -NMR (top) and  $^{19}\text{F}$ -NMR (bottom) spectra of  $\text{C}_{12}\text{-SO}_2\text{F}$

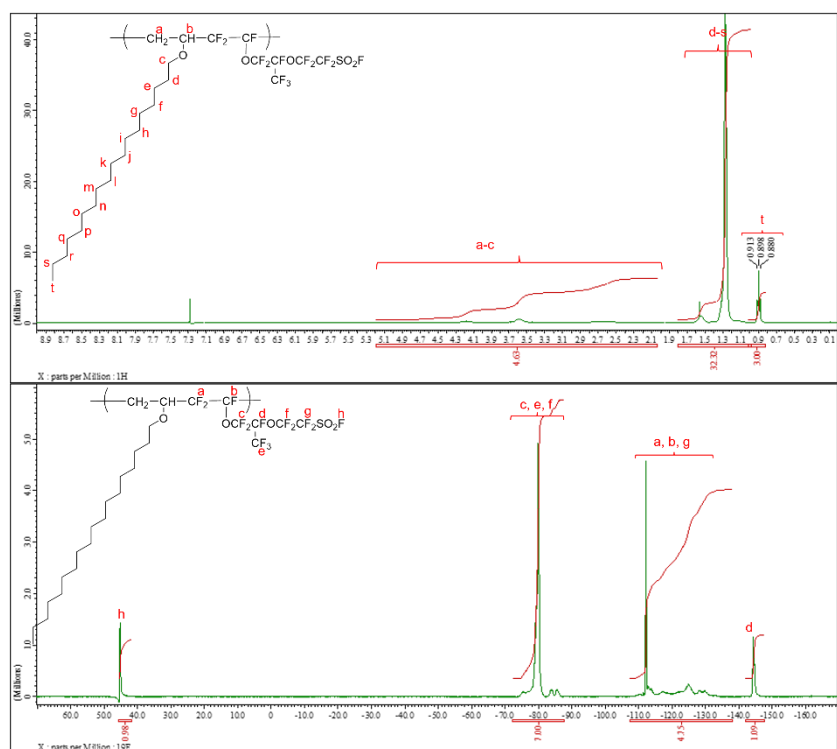


Figure S4.  $^1\text{H}$ -NMR (top) and  $^{19}\text{F}$ -NMR (bottom) spectra of  $\text{C}_{18}\text{-SO}_2\text{F}$

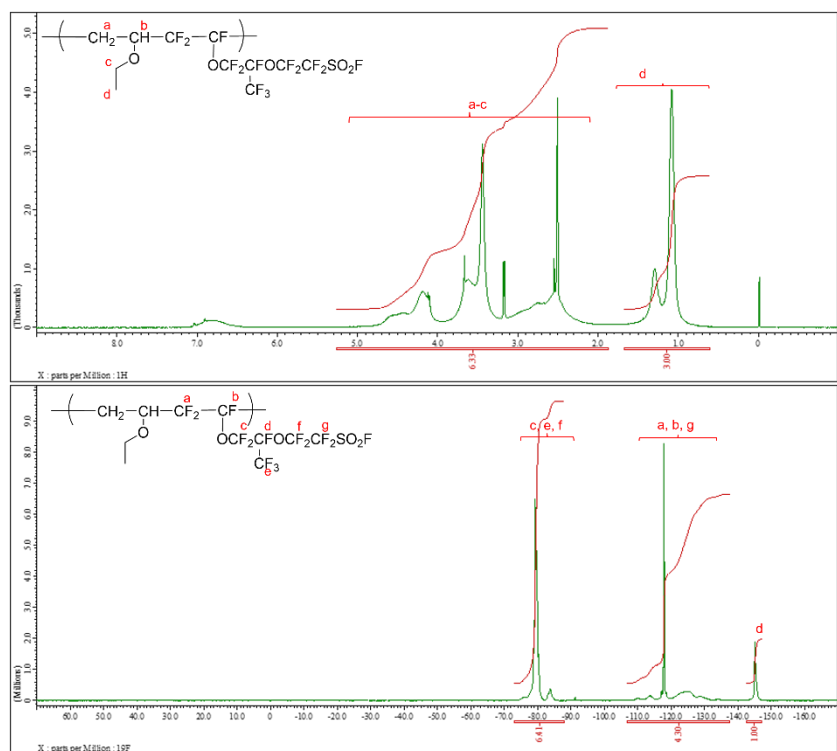


Figure S5.  $^1\text{H}$ -NMR (top) and  $^{19}\text{F}$ -NMR (bottom) spectra of  $\text{C}_2\text{-SO}_3\text{Li}$

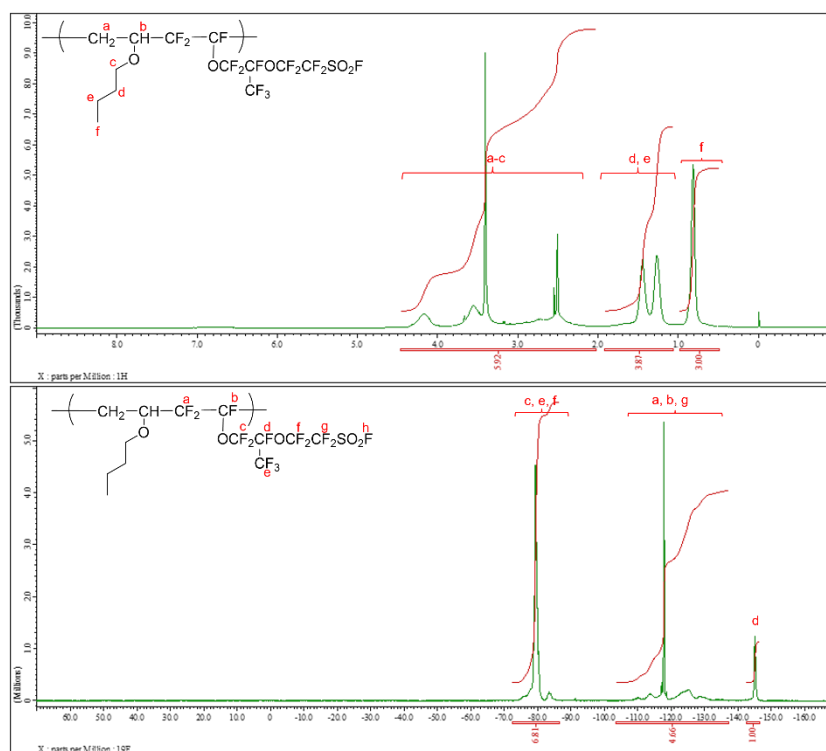


Figure S6.  $^1\text{H}$ -NMR (top) and  $^{19}\text{F}$ -NMR (bottom) spectra of  $\text{C}_4\text{-SO}_3\text{Li}$

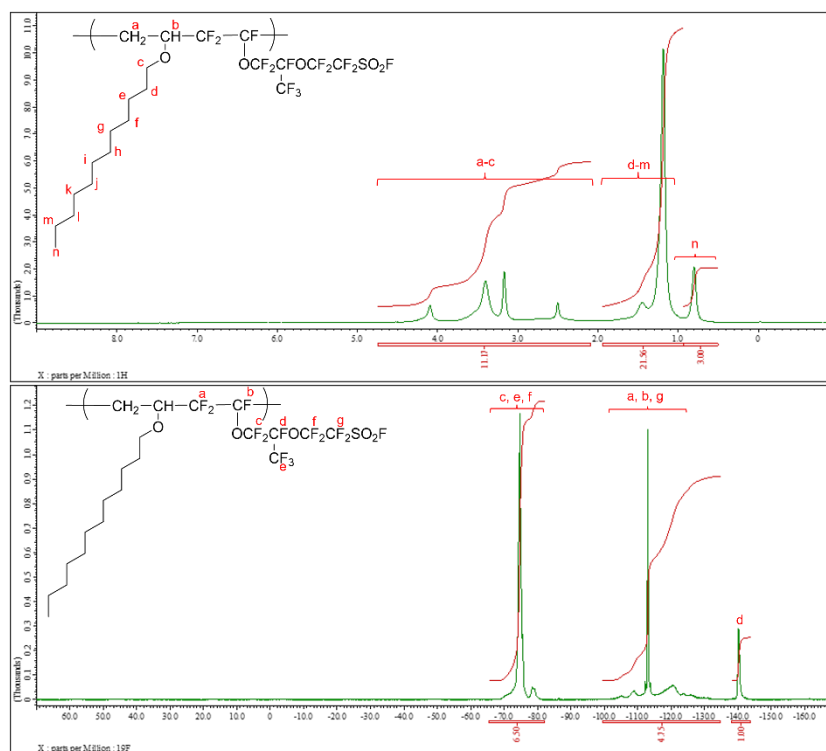


Figure S7.  $^1\text{H}$ -NMR (top) and  $^{19}\text{F}$ -NMR (bottom) spectra of  $\text{C}_{12}\text{-SO}_3\text{Li}$

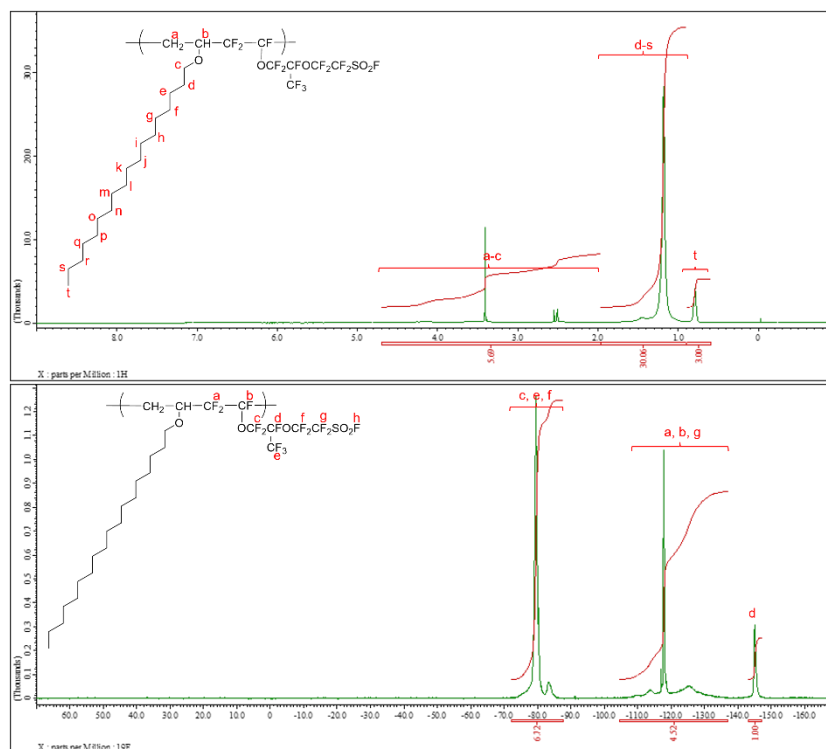


Figure S8.  $^1\text{H}$ -NMR (top) and  $^{19}\text{F}$ -NMR (bottom) spectra of  $\text{C}_{18}\text{-SO}_3\text{Li}$

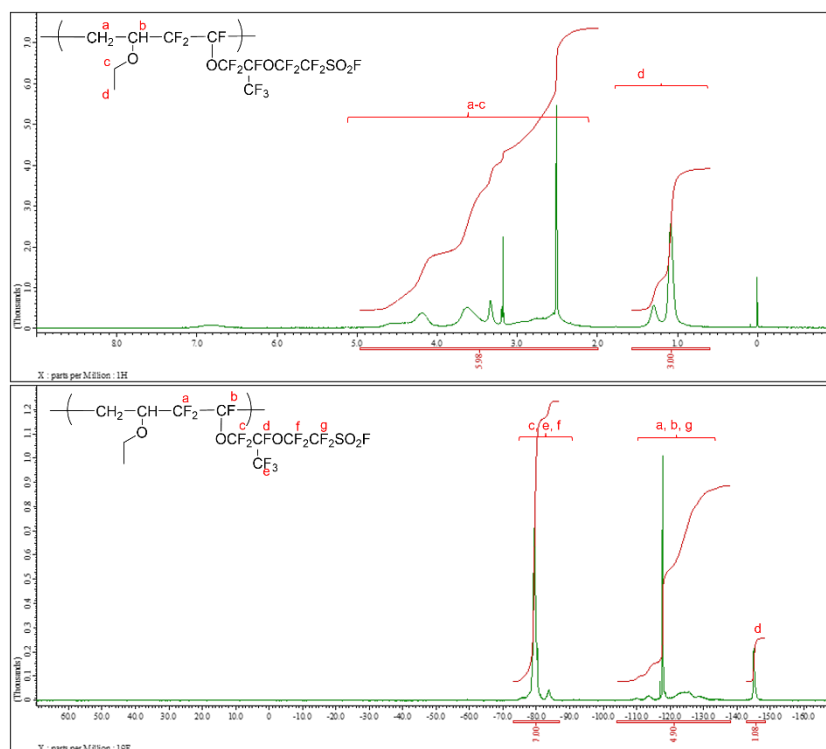


Figure S9.  $^1\text{H}$ -NMR (top) and  $^{19}\text{F}$ -NMR (bottom) spectra of  $\text{C}_2\text{-SO}_3\text{Cs}$

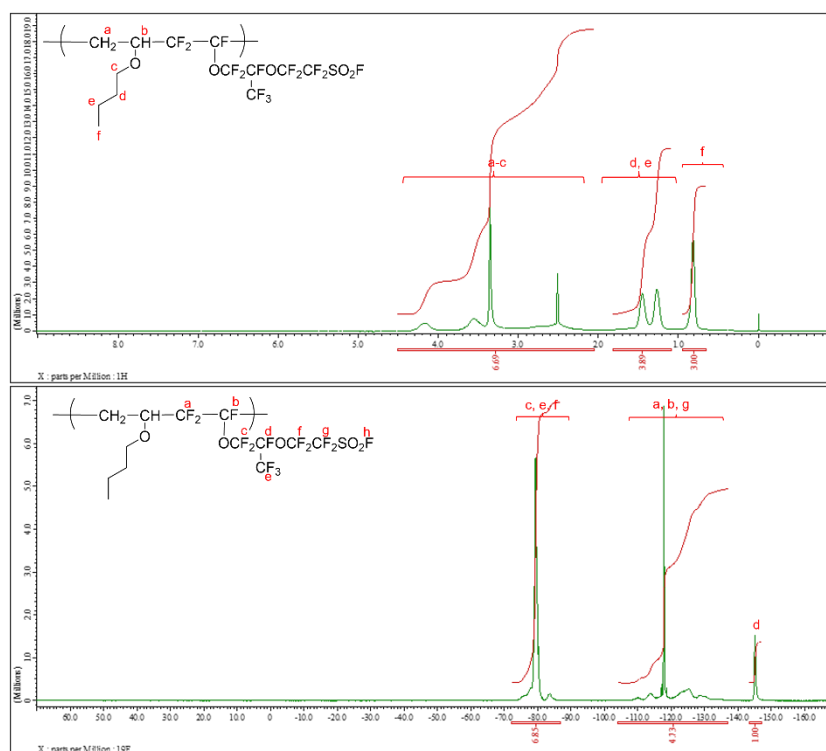


Figure S10.  $^1\text{H}$ -NMR (top) and  $^{19}\text{F}$ -NMR (bottom) spectra of  $\text{C}_4\text{-SO}_3\text{Cs}$

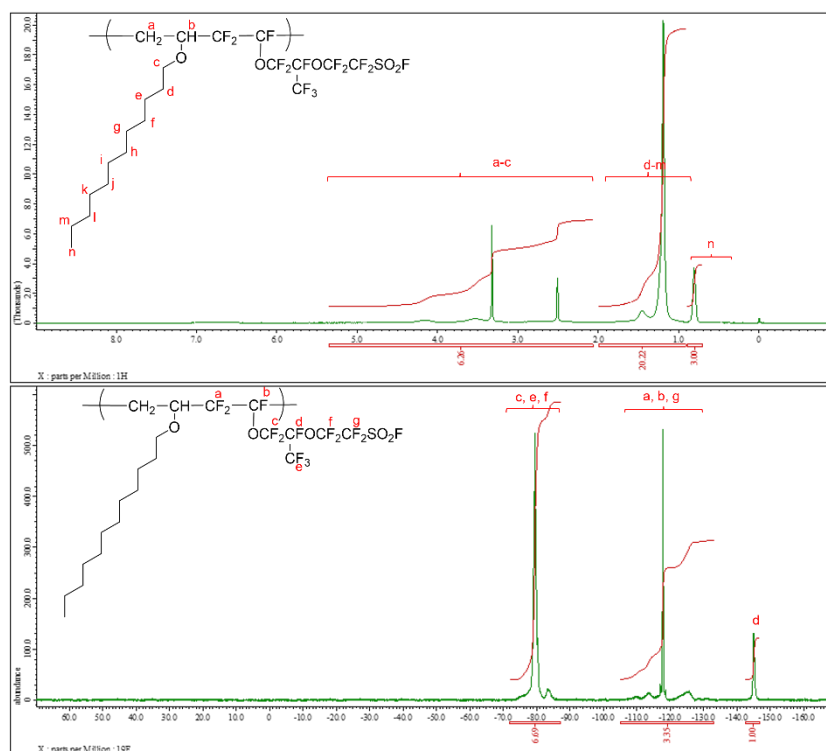


Figure S11.  $^1\text{H}$ -NMR (top) and  $^{19}\text{F}$ -NMR (bottom) spectra of  $\text{C}_{12}\text{-SO}_3\text{Cs}$

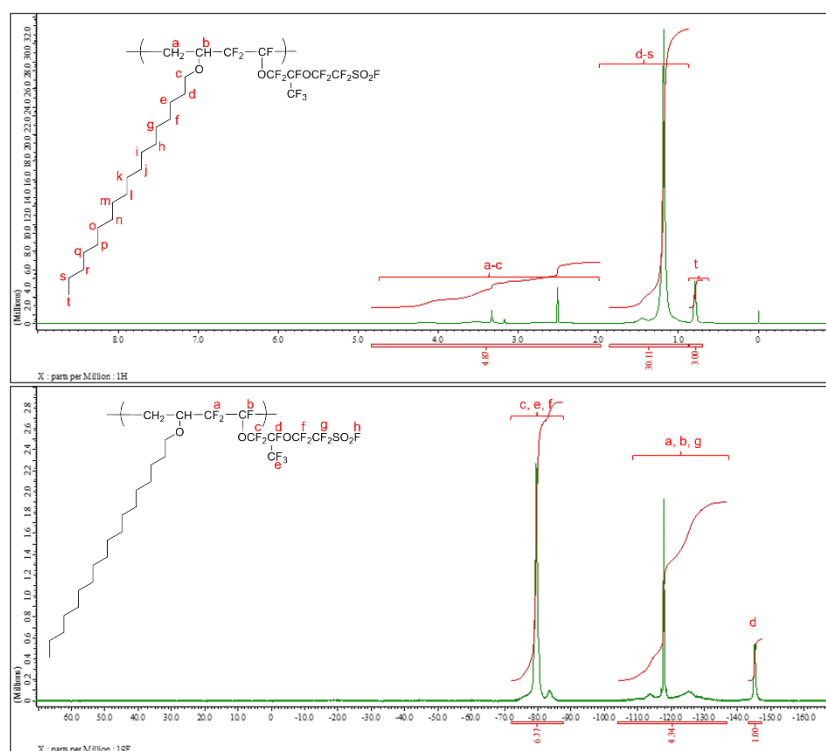


Figure S12.  $^1\text{H}$ -NMR (top) and  $^{19}\text{F}$ -NMR (bottom) spectra of  $\text{C}_{18}\text{-SO}_3\text{Cs}$

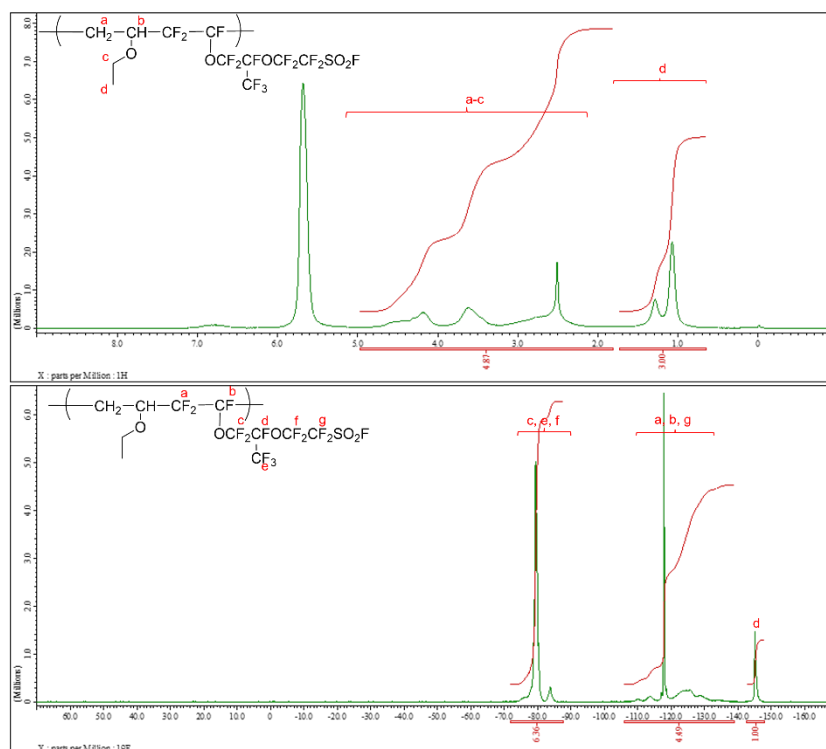


Figure S13.  $^1\text{H}$ -NMR (top) and  $^{19}\text{F}$ -NMR (bottom) spectra of  $\text{C}_2\text{-SO}_3\text{H}$



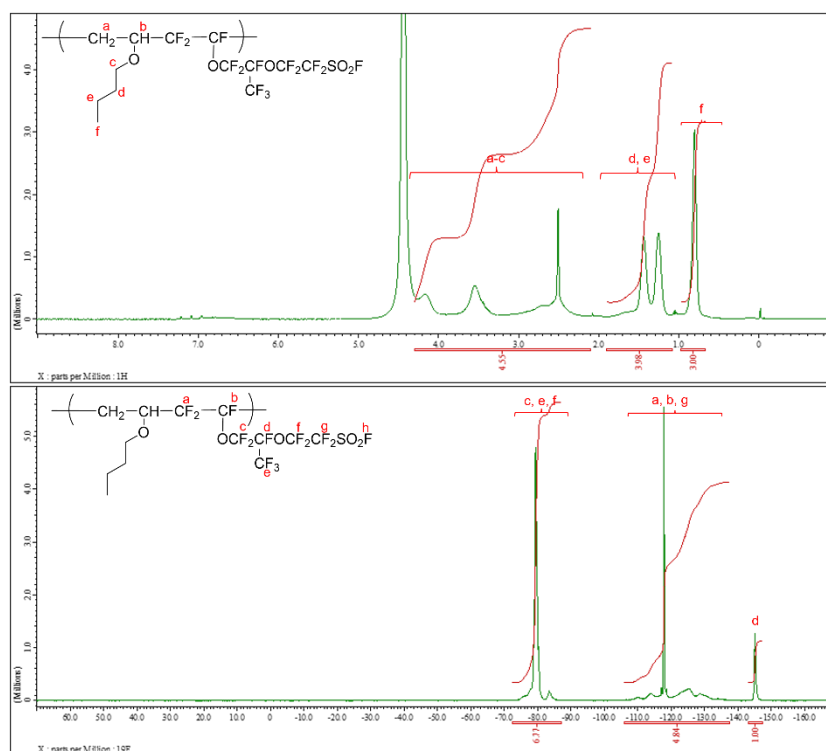


Figure S14.  $^1\text{H}$ -NMR (top) and  $^{19}\text{F}$ -NMR (bottom) spectra of  $\text{C}_4\text{-SO}_3\text{H}$

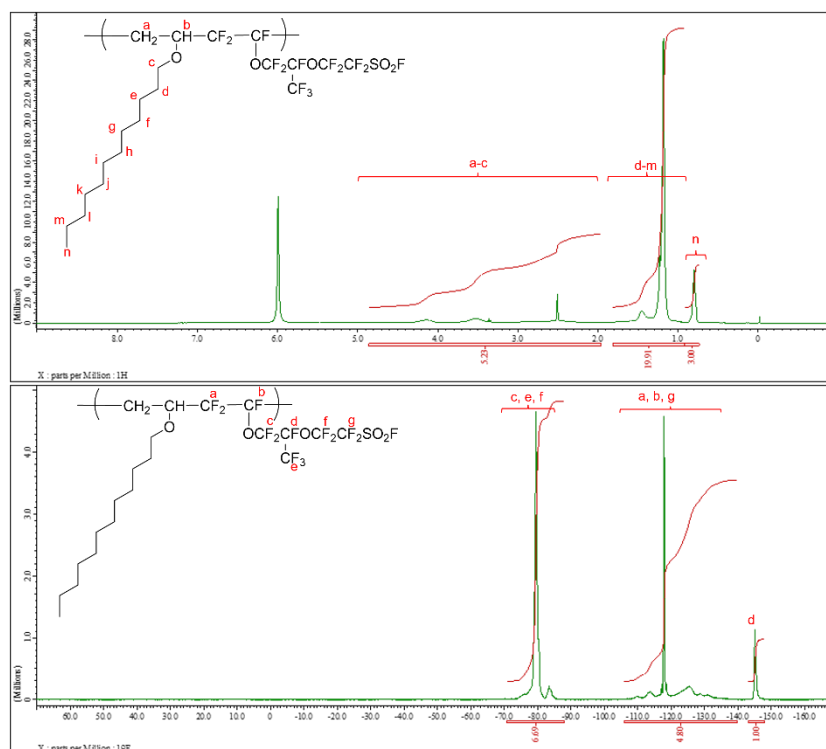


Figure S15.  $^1\text{H}$ -NMR (top) and  $^{19}\text{F}$ -NMR (bottom) spectra of  $\text{C}_{12}\text{-SO}_3\text{H}$

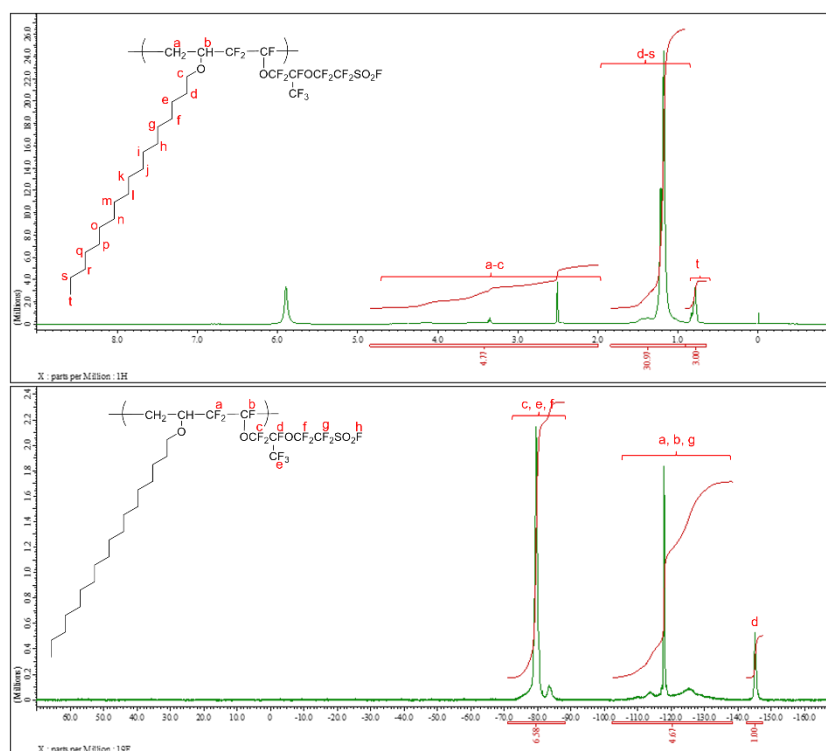


Figure S16. <sup>1</sup>H-NMR (top) and <sup>19</sup>F-NMR (bottom) spectra of C<sub>18</sub>-SO<sub>3</sub>H

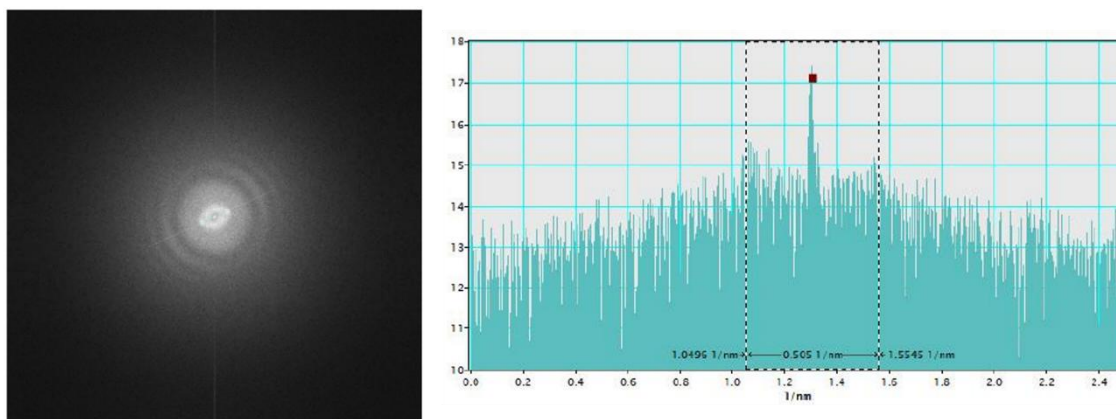


Figure S17. 2D Fourier transfer of TEM bright field image (right) and its strength profile (left) of C<sub>12</sub>-SO<sub>3</sub>Li

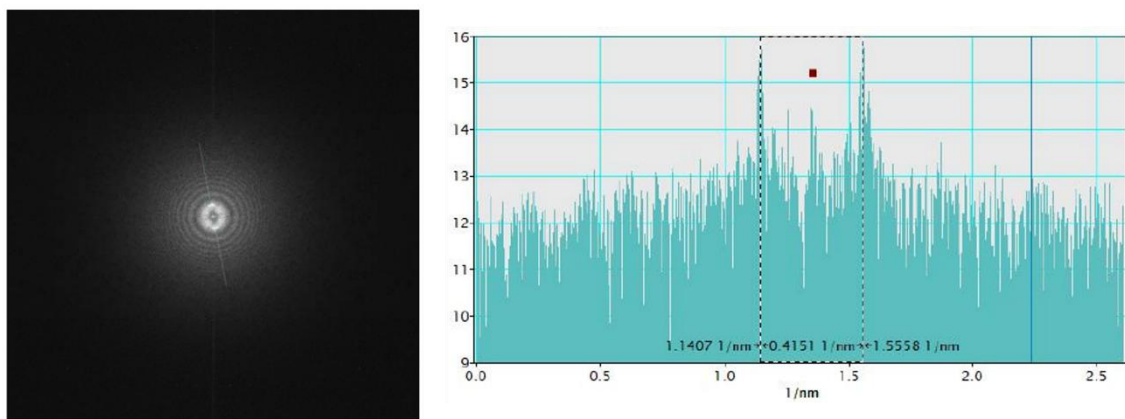


Figure S18. 2D Fourier transfer of TEM bright field image (right) and its strength profile (left) of C<sub>12</sub>-SO<sub>3</sub>Li

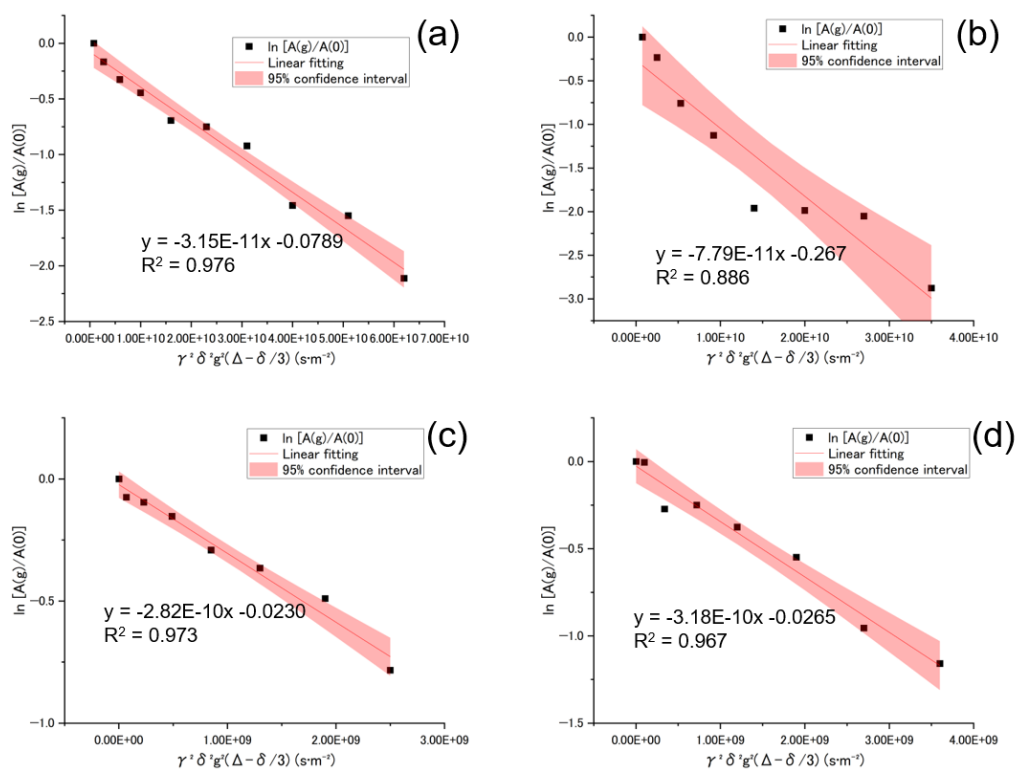


Figure S19. PFG-NMR diffusion plot of C<sub>2</sub>-SO<sub>3</sub>H (a), C<sub>4</sub>-SO<sub>3</sub>H (b), C<sub>12</sub>-SO<sub>3</sub>H (c) and C<sub>18</sub>-SO<sub>3</sub>H (d)